



# Effect of Mesh Wettability Modification on Atmospheric and Industrial Fog Harvesting

Jong Hoon Kang<sup>1</sup>, Jeong-Won Lee<sup>2</sup>, Ji Yeon Kim<sup>2</sup>, Jong Woon Moon<sup>2</sup>, Hyeon Seo Jang<sup>2</sup> and Sung Yong Jung<sup>2\*</sup>

<sup>1</sup> POSCO, Technical Research Laboratories, Iron and Steel Process Engineering Research Group, Pohang-si, South Korea,

<sup>2</sup> Department of Mechanical Engineering, Chosun University, Gwangju, South Korea

## OPEN ACCESS

### Edited by:

Umberto Lucia,  
Politecnico di Torino, Italy

### Reviewed by:

Ranjan Ganguly,  
Jadavpur University, India  
Saeid Azizian,  
Bu-Ali Sina University, Iran

### \*Correspondence:

Sung Yong Jung  
syjung@chosun.ac.kr

### Specialty section:

This article was submitted to  
Interdisciplinary Physics,  
a section of the journal  
Frontiers in Physics

**Received:** 16 March 2021

**Accepted:** 26 April 2021

**Published:** 24 May 2021

### Citation:

Kang JH, Lee J-W, Kim JY, Moon JW, Jang HS and Jung SY (2021) Effect of Mesh Wettability Modification on Atmospheric and Industrial Fog Harvesting. *Front. Phys.* 9:680641. doi: 10.3389/fphy.2021.680641

Freshwater shortage has been receiving considerable attention, and water harvesting is one of the potential solutions to this water crisis. Several researchers have tried to improve the harvesting capabilities by changing mesh wettability for atmospheric fog harvesting. However, the wettability effect on water harvesting from white plumes has not yet been investigated thoroughly, despite industrial cooling towers being considered as alternative water resources, because of the large amounts of fog plumes generated. In this study, surface wettability was modified with a robust and simple method for practical scaled-up applications, and we explored the influence of mesh wettability on atmospheric and industrial fog harvesting. In atmospheric fog harvesting, both superhydrophilic meshes (SHPMs), and superhydrophobic meshes (SHBMs) were found to improve the harvesting performance, with superhydrophobic treatments providing the best collection efficiency. In contrast, only superhydrophilicity improves the performance in industrial fog harvesting with flat mesh screens. We hypothesize that this research will be useful for mesh design, as it analyzes the influence of mesh wettability on the performance of water collection in both atmospheric and industrial water harvesting.

**Keywords:** water harvesting, industrial fog harvesting, surface wettability modification, collection efficiency, atmospheric fog harvesting

## INTRODUCTION

With the depletion of energy resources, the global crisis regarding freshwater scarcity has received significant attention in both arid and humid environments [1]. In addition to being indispensable for life and well-being (used in household living and irrigation), freshwater is essential in several industries, including thermal power plants and steel-making factories [2]. To acknowledge the significance of this water crisis, the UN announced the period of 2005–2015 as the International Decade for Action “Water for Life” [3], and UNESCO marked 2013 as the International Year for Water Cooperation [4]. Harvesting water to provide a source of good-quality freshwater is one of the potential solutions to the water crisis [5].

Two typical methods have been employed for water harvesting. The first is dew harvesting, wherein water is collected from the phase change of water vapor to liquid, followed by transportation [6–8]. For the nucleation of water vapor on a surface, the surface temperature of a substrate must be lower than that of the surrounding temperature [9].

Therefore, dew harvesting frequently requires active cooling of the surface, which requires energy input. The second method is fog harvesting, which collects water from fog-laden flows [10, 11]. In contrast to dew harvesting, fog harvesting collects water without using any additional energy. Fog harvesting follows a two-step process for obtaining water. The first step is fog droplet deposition on a solid surface, which depends strongly on the aerodynamics of the mesh used [12, 13]. The aerodynamics of the mesh are related to two variables: the ratio ( $R^* = r_{\text{fog}}/R$ ) of the droplet radius ( $r_{\text{fog}}$ ) to the wire radius ( $R$ ) and the shading coefficient (SC). The second step is the transport of the deposited liquid to a reservoir. To improve drainage, it is necessary to reduce the loss of captured droplets through evaporation and/or re-entrainment into the fog-laden flow.

To enhance the efficiency of water harvesting, the effects of mesh topology and surface chemistry have been investigated in many studies. Park et al. [12] investigated the SC,  $R^*$ , and surface wettability and proposed a theoretical model to predict the capture efficiency. By conducting a single vertical superhydrophilic wire experiment, Jiang et al. [14] examined the empirical correlation between the correction rate and the Stokes number. Raschel meshes were reported to be feasible for efficient fog collection in pilot studies [15–17], and the possibility of enhancing fog collection through modifications of surface wettability and geometrical parameters was investigated [18]. The desirable surface wettability parameters, such as hydrophilicity and hydrophobicity, were reported to depend on the water-harvesting conditions, such as dew and fog harvesting [19]. The overall efficiency of water harvesting was determined by the relative importance of the capturing-efficiency and the removal-efficiency. By mimicking various plants and animals, various surfaces that modified the surface wettability were developed [20–24]; for example, the modifications of mixed wettability and fiber size variations were based on the back of a beetle and cactus spine, respectively. These studies showed that the hybrid wettability substrates have better performance than uniform wetting coated surfaces. Almost all of the hybrid surfaces were formed on plate surfaces by using plasma or masking, but it is difficult to apply this method for meshes. In addition, those methods have scale-up issues in practical applications. The form of Janus Copper, suggested by Zhou et al. [25], having porous hybrid wetting surfaces also suffered from the scaling issue.

Double-layered woven polyolefin Raschel meshes have been used in numerous field studies and exhibit good collection efficiency [15–17]. However, their water-harvesting performances vary according to their properties. Moreover, it is difficult to create a double layer with similar SCs and to purchase Raschel meshes with the same dimensions and surface wettability for fog harvesting in different countries. In addition, these polymer meshes have a serious problem in terms of sustainability because they can be torn by strong winds. Therefore, many researchers have attempted to solve these issues by replacing the mesh material with commercial metal meshes with improved fog harvesting capabilities produced by modifying the surface wettability of the metal meshes [12]. Although the effectiveness of such surface modifications has been validated in laboratory-scale tests, several methods of surface coatings are not suitable

for practical use, owing to the changes in their wettability characteristics caused by contamination.

Most studies on the effects of surface coatings on water harvesting have focused on fog capture under atmospheric water-harvesting situations. Industrial cooling towers in thermal power plants and steel-making factories have a large potential for water harvesting because cooling towers generate large amounts of fog plumes because of the evaporation of the cooling water. In addition to the economic and renewable aspects, white plumes from cooling towers have recently received considerable attention from environmental perspectives [2, 26]. Although cooling towers in industries are alternative water-harvesting resources and it is known that the performance depends on the wettability of meshes [27], research on the applicability of the wettability modification of commercial metal meshes in fog harvesting from industrial white plumes is not enough, and cheaper wettability modified methods, such as chemical material and process complexity, are required for practical scaled-up applications.

In this study, the feasibility of surface wettability modifications for practical scaled-up applications is investigated experimentally to improve water harvesting in both atmospheric and industrial scenarios. The surface wettability is changed by the developing hierarchical micro/nanostructures on surfaces, which is known to be a robust and simple method. Superhydrophilic meshes (SHPMs) and superhydrophobic meshes (SHBMs) are fabricated from commercial aluminum meshes, and the performances of these meshes with different surface wettability characteristics are compared for simulated atmospheric and industrial fog harvesting.

## MATERIALS AND METHODS

### Fabrication of Surface-Modified Mesh

Two commercial aluminum meshes (Goodfellow, Huntingdon, UK) were used as the base meshes (BM). The specifications of the BMs are summarized in **Table 1**. Porosity is the fraction of projected area occupied by the space and the SC and is expressed as 1. The BMs were dipped in 1 M sodium hydroxide (NaOH, bead, 98.0%, Samchun Chemical, Seoul, Republic of Korea) solution at 25°C for 1 min, and the residual solution was removed with deionized water (DI water). Thereafter, the meshes were etched in 2 M hydrochloric acid (HCl, 35.0–37%, Samchun Chemical, Seoul, Republic of Korea) solution at 25°C for 5 min. The etched meshes were cleaned with DI water. Subsequently, the meshes were immersed in NaOH solution for 5 s and in hot DI water (above 90°C) for 10 min, before being dried in an oven at 60°C. Through this process, SHPMs were obtained. The SHBM was fabricated by soaking one SHPM for 10 min in a solution of normal hexane (n-hexane, 96%, Samchun Chemical, Seoul, Republic of Korea) mixed with 0.1% v/v heptadecafluoro-1,1,2,2-tetrahydrodecyl trichlorosilane ( $\text{C}_{10}\text{H}_4\text{C}_{13}\text{F}_{17}\text{Si}$ , HDFS, Gelest) for fluorination. After fluorination, the SHBM was dried in an oven at 175°C. The process has been described in detail in a previous study [28].

## Characterization of Fabricated Mesh

The surface structures of the meshes were examined using field-emission scanning electron microscopy (FE-SEM, S-4800, Hitachi, Tokyo, Japan), and images were obtained at an acceleration voltage of 15 kV. The static contact angles on the fabricated meshes were measured using a drop shape analysis system (Phoenix 300 Touch, SEO). A 5-ml droplet of distilled water was used for contact angle measurements. The contact angles were averaged over at least 10 readings at different locations on each specimen at 25°C.

## Scaled-Down Atmospheric Fog Harvesting

**Figure 1** shows the experimental configurations for simulated atmospheric fog harvesting. The apparatus was composed of a humidifier for fog generation, a fan, and two concentric acrylic cylinders with diameters of 100 and 60 mm, respectively. The sizes of the mesh samples were the same as that of the inner cylinder. The fog collection amount was strongly influenced by the air stream velocity ( $V_0$ ), which was controlled by the voltage applied to the fan and the distance ( $s$ ) between the mesh and the fog tube. In all experiments,  $s$  and  $V_0$  were fixed at 10 mm and 1.7 m/s, respectively. The amount of fog generated ( $W_{gen}$ ) was calculated by measuring the reduction in the weight of the humidifier. The harvested water ( $W_{coll}$ ) was collected in a reservoir located under a mesh sample, and the amount of water collected was determined by measuring the increase in the weight of the reservoir. Changes in both weights were measured every 5 min for 30 min. The measurement values of at least three consecutive experiments

were averaged. To check the durability, the performances were measured at an interval of 1 week after exposure to surrounding environments.

## Scaled-Down Industry Fog Harvesting

**Figure 2B** shows the white plumes near a cooling tower in a steel-making factory. The apparatus for industry fog harvesting was designed by scaling down this cooling tower. The image and schematic diagram are shown in **Figures 2A,C**, respectively. **Figure 2A** represents the setup of a scaled-down version of the actual cooling tower as shown in **Figure 2B**. The droplets having a size of  $\sim 5\ \mu\text{m}$  were generated using a standard ultrasonic humidifier with tap water. It is known that the size of droplets that cannot be captured by traditional drift eliminators in industrial cooling towers is  $<40\ \mu\text{m}$ . A large number of those droplets have a size smaller than  $5\ \mu\text{m}$  [29]. Therefore, our generation method had successfully mimicked the fog droplet distributions, taking into account the potential application of the present study. The generated droplets were blown to the vertical channel by direct current (DC) fan after collecting at the manifold to achieve the supersaturation condition. This is similar to the occurrence of the white plume near a cooling tower in a steel-making factory, as shown in **Figure 2B**. Square meshes were prepared with a width of 56.25 mm, which was 0.75 times more than that of the tower outlet. Each sample mesh was positioned at 2 cm ( $H$  in **Figure 2C**) above the exit plane of the tower. In addition to the effect of surface wettability, an inclination angle ( $\theta$ ) effect was also observed. The inclination angle ( $\theta$ ) was varied from 15 to 75°, at an angular interval of 15°. Only a portion of the mesh samples, which is marked in **Figure 2C**, was located inside a virtual vertical cylinder above the tower outlet. Water was collected in a reservoir located around the tower outlet. The amount of water collected was measured after 5 h. The measurement values of at least three consecutive experiments were also averaged using data obtained at the interval of 1 week after exposure to surrounding environments.

**TABLE 1** | Specifications of base meshes used in this study.

| Mesh | Wire diameter ( $2R$ , mm) | Opening ( $2D$ , mm) | Porosity (%) |
|------|----------------------------|----------------------|--------------|
| #20  | 0.4064                     | 0.8636               | 46           |
| #40  | 0.254                      | 0.381                | 36           |

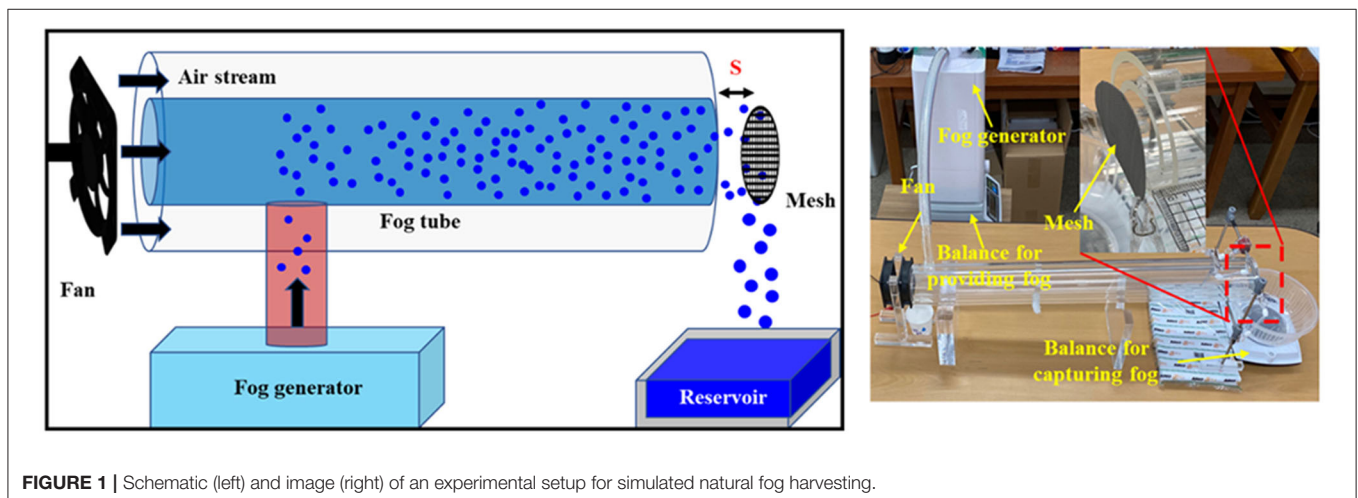
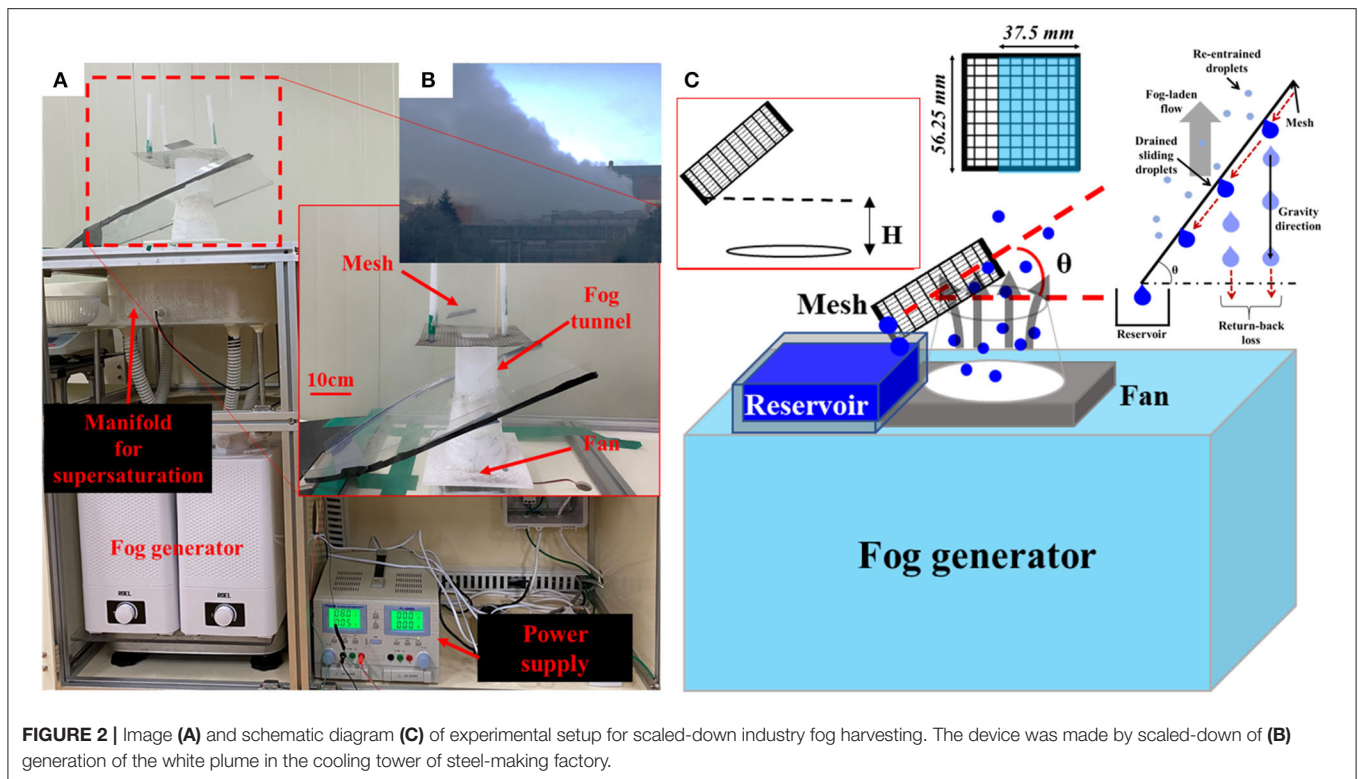


**FIGURE 1** | Schematic (left) and image (right) of an experimental setup for simulated natural fog harvesting.



## RESULTS AND DISCUSSION

### Characteristics of Surface-Modified Mesh

**Figure 3** shows SEM images of the mesh surface during the surface modification process. After etching with HCl, microstructures were formed on the aluminum surfaces of the mesh wires. Hierarchical micro/nanostructures were created after treatments with NaOH solution and hot water (SHPM). When the microstructure is formed, there is no change in the aluminum surface composition, but aluminum hydroxide ( $\text{Al}(\text{OH})_3$ ) is formed simultaneously with the nanostructure [30]. Without changing the surface micro/nanostructures, SHBM was finally obtained by applying an HDFS self-assembled monolayer (SAM) coating, lowering the surface energy. To confirm the modification of surface wettability, consecutive images of water droplets falling on the SHPM and SHBM were obtained, as shown in **Figure 4**. The water droplets exhibited fan-cake shapes, and the boundary of wetting was extended after falling on the SHPM. In contrast, the water droplets maintained their spherical shapes and performed sliding motions on the SHBM even when the inclined angle was almost zero. These droplet shapes, wetting, and sliding indicated that the superhydrophilic and superhydrophobic surfaces were well-formed.

The detailed wettability of the meshes was characterized by measuring the contact angles, as shown in **Figure 5**. The #20 BM had a contact angle similar to that of a normal smooth aluminum surface, which exhibited slight hydrophilicity [31]. In finer meshes (#40 BM), the contact angle became larger, although the meshes were made of the same materials.

The contact angles of the SHPMs were lower than  $10^\circ$  because of the increase in surface roughness after forming micro/nanostructures, inducing the Wenzel state. The wettability of SHBMs changed to hydrophobicity after the HDFS SAM coating because water droplets could not penetrate the air pocket inducing the Cassie state. Surfaces with contact angles  $> 150^\circ$  are classified as superhydrophobic surfaces. The SHBMs, in this study, had contact angles lower than this criterion. These measured lower contact angles were caused by the mesh structures, which strongly affected the determination of the base and contact lines during the contact angle measurements. The baselines were decided by choosing a location midway between the apexes and valleys. Even though the static contact angle values were lower than  $150^\circ$  the apexes and valleys, caused by the mesh structures, which strongly affect superhydrophobic surfaces, as shown in **Figure 4**. In addition, the contact angle on a superhydrophobic smooth surface was also represented to confirm the superhydrophobic modification. Therefore, meshes after SAM coating can be classified as superhydrophobic. Advancing and receding contact angles measured by the tilting method are  $148.0^\circ \pm 1.4$  and  $137.2^\circ \pm 1.1$  for the #40 SHBM, respectively. The #20 SHBM has advancing and receding contact angles of  $144.4^\circ \pm 1.3$  and  $135.6^\circ \pm 1.2$ , respectively.

### Performance in Atmospheric Fog Harvesting

**Figure 6** shows the time variations of the collected water amount. The total weight of water collected was divided by the mesh

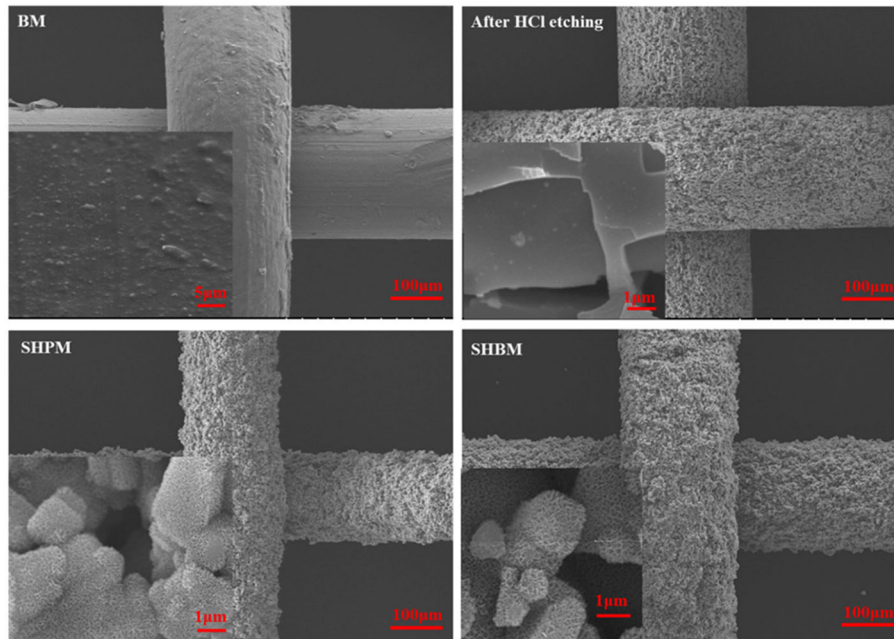


**FIGURE 3** | Scanning electron microscopy (SEM) images of tested #40 meshes. Formations of micro and nanostructures are observed after HCl etching and NaOH solution treatment, respectively.

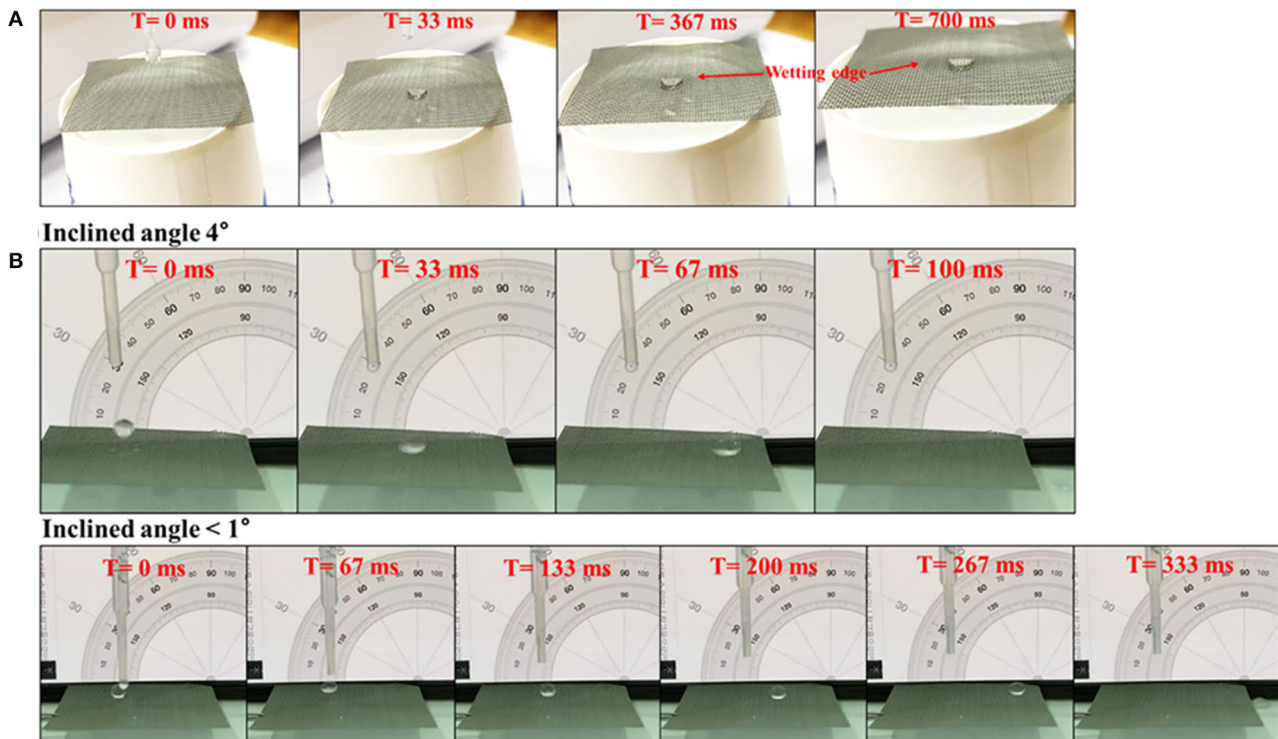


**FIGURE 4** | Consecutive images of falling droplet wetting and sliding on (A) SHPM and (B) SHBM, respectively.

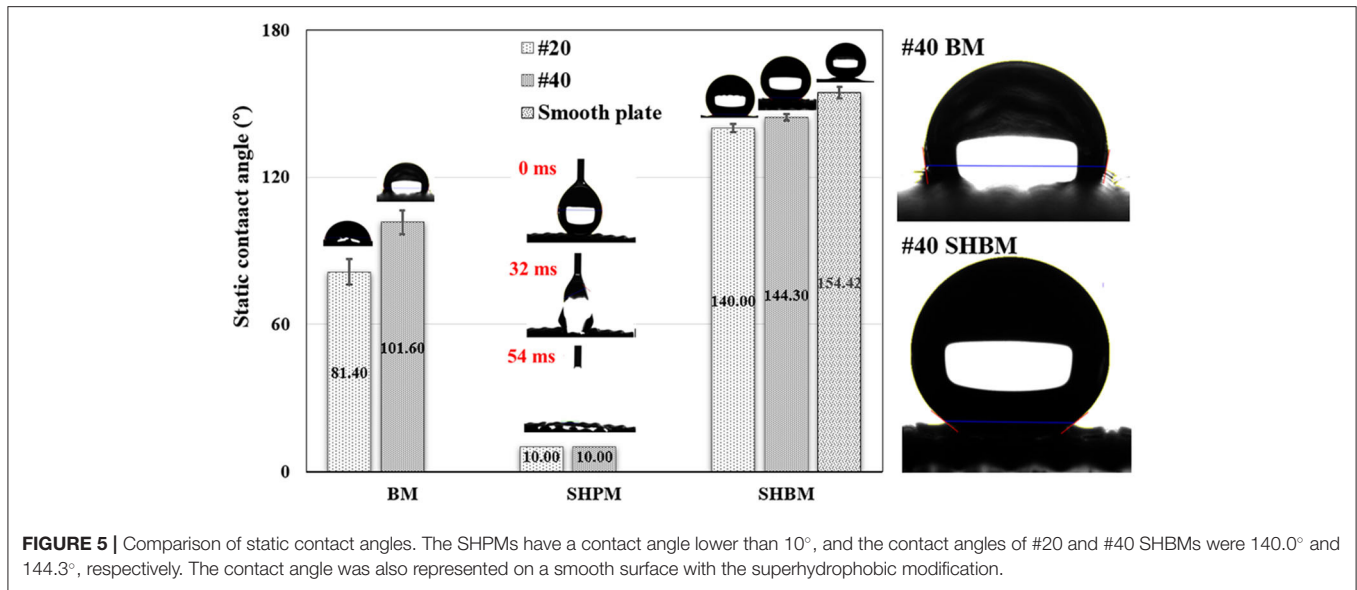


**FIGURE 5 |** Comparison of static contact angles. The SHPMs have a contact angle lower than 10°, and the contact angles of #20 and #40 SHBMs were 140.0° and 144.3°, respectively. The contact angle was also represented on a smooth surface with the superhydrophobic modification.

area. In all the cases, the collected amounts reached a steady-state within a short time (5 min in this study), and the amounts increased linearly over time. Therefore, the measurement for 30 min was sufficient to evaluate the collection performance. Compared to BM, both SHPM and SHBM had larger slopes. This meant that both the SHPM and SHBM showed an improvement in the collection performance in atmospheric fog harvesting.

The overall fog collection efficiency is the product of the aerodynamic collection efficiency ( $\eta_a$ ), capture efficiency ( $\eta_c$ ), and draining efficiency ( $\eta_d$ ) [32].

$$\eta = \eta_a \cdot \eta_c \cdot \eta_d \tag{1}$$

$\eta_a$  is the fraction of droplets that collide with the solid portion of the mesh. The theoretical model for  $\eta_a$  was proposed by Rivera [32] and is expressed as shown:

$$\eta_a = \frac{SC}{1 + \sqrt{\frac{C_0}{C_D}}} \tag{2}$$

where  $C_D$  is the drag coefficient of an entire mesh structure and is independent of SC.  $C_D$  is a function of the Reynolds number (Re) and structure. Based on the mesh diameter, the corresponding Re was 6,750. In atmospheric fog harvesting experiments, the mesh was a circular disk with  $C_D$  as 1.1 for the tested Re condition [33]. In contrast,  $C_0$  is the pressure loss coefficient for a mesh, and it depends on the SC. For a wire mesh, the correlation for  $C_0$  given by Rivera is expressed as

$$C_0 = 1.3SC + \left( \frac{SC}{1 - SC} \right)^2 \tag{3}$$

$C_0$  of the #20 and #40 meshes were 2.05 and 3.99, respectively. From the Equation (2), the theoretical  $\eta_a$  was 22.7 and 22.0%

for the #20 and #40 meshes, respectively. This  $\eta_a$  was not influenced by the surface modifications according to Equations (2, 3) as the entire structure and SC did not change after the modifications. Therefore, the changes in mesh wettability induced an improvement in  $\eta_c$  and  $\eta_d$ .

The performances of the tested mesh samples were compared in Figure 7. The water collection efficiency was calculated to evaluate the performance. The overall water collection efficiency was calculated as

$$\eta = \frac{W_{coll}}{W_{gen}} \tag{4}$$

Compared with #20 BM, #40 BM had slightly lower theoretical  $\eta_a$ , but provided slightly better performance in atmospheric water harvesting. As denoted in Equation (1), the overall efficiency depended on  $\eta_c$  and  $\eta_d$ , in addition to  $\eta_a$ . With the same wind velocity and fog droplet size, the deposited fraction of fog droplets hitting wires increases as  $R^*$  increases [12]. Therefore, a larger  $R^*$  of #40 led to a higher  $\eta$  than that of #20, which had higher  $\eta_a$ .

Compared with BMs, SHPMs and SHBMs had higher collection efficiencies, as shown in Figure 7. Two typical adverse phenomena of water harvesting were the loss of deposited droplets (re-entrainment) and the clogging of meshes [12]. The re-entrainment occurs when the drag force is higher than the adhesion force. The clogging depends on the relative magnitude of gravity and pinning forces. As the contact angle increases, the adhesion force decreases. This causes the increase and decrease of re-entrainment and clogging possibilities. Clogging related to gravity and pinning forces modified the local aerodynamics. Figures 8A–C show the droplets dispensed on vertically placed #40 meshes. Dispensed droplets had different interactions with meshes. Droplets on BM were pinned, and they maintained a hemispherical shape. Droplets on SHPM completely wetted

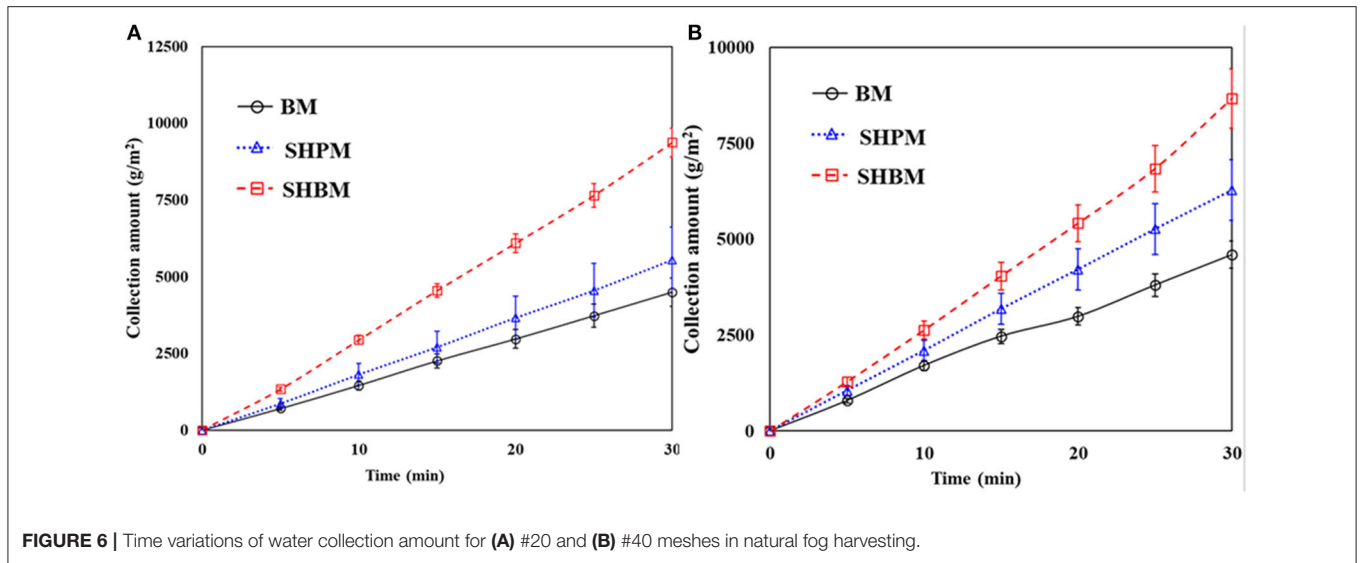


FIGURE 6 | Time variations of water collection amount for (A) #20 and (B) #40 meshes in natural fog harvesting.

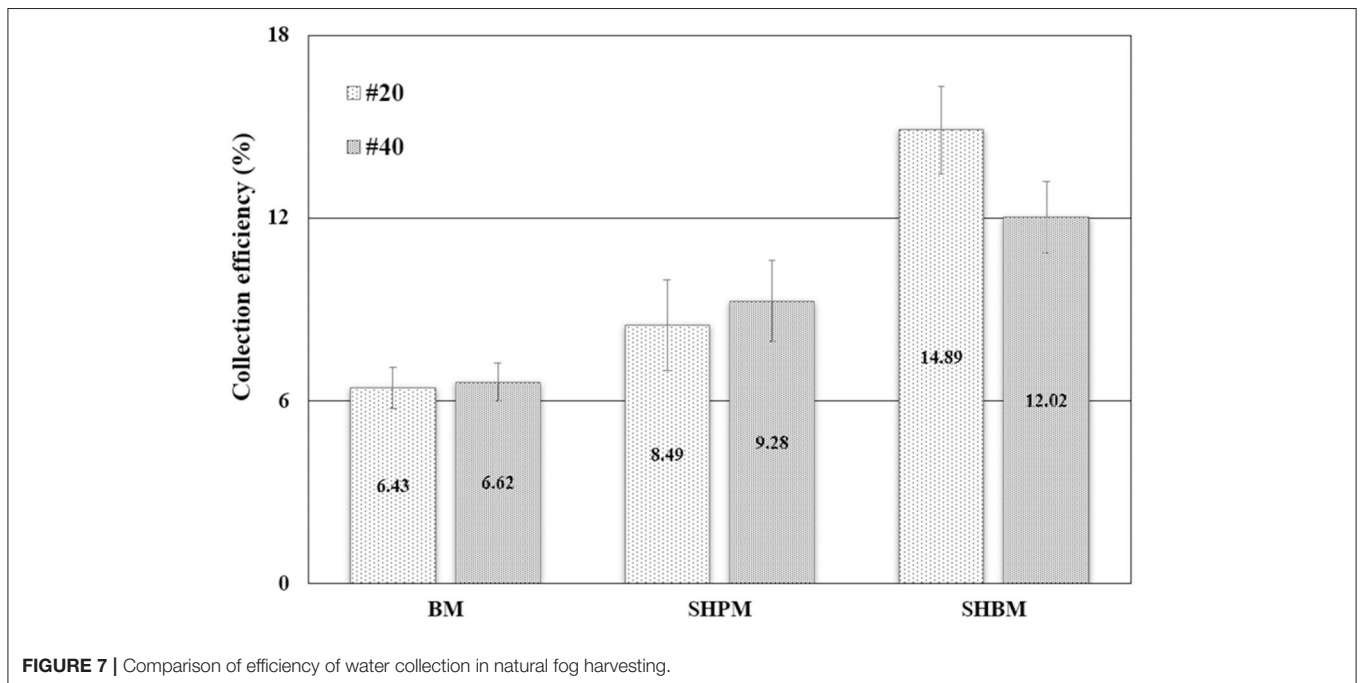
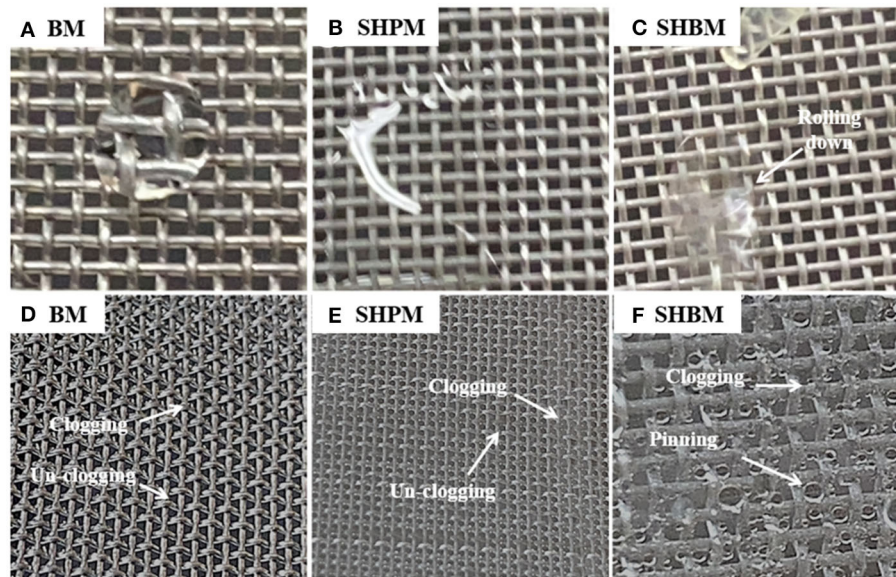


FIGURE 7 | Comparison of efficiency of water collection in natural fog harvesting.

and blocked the pores. The clogged water in SHPM attracted droplets, grew faster, and was drained (**Supplementary Video 2**). As shown in **Figures 8D,F**, the droplets in SHPM fully occluded pores, whereas clogged droplets in BM were hung at corners between wires. Dispensed droplets on SHBM rolled down without any attachments (**Supplementary Video 3**). In the atmospheric fog harvesting with SHBM, clogging also occurred because droplets were smaller than those dispensed in **Figures 8A–C**. Different from clogged droplets in BM and SHPM, the clogged droplets in SHBM were partially suspended

and had an almost spherical shape, resulting in a small adhesion force.

The superhydrophobic treatment was found to be the most effective, and the collection performance improved approximately by two times. No clogging occurred on the SHBMs, and this clogging protection provided better water harvesting. After surface modification with SHBM, the water collecting performances of the #20 and #40 BMs were reversed. The re-entrainment depending on the drag and adhesion forces is a function of the contact angle, and the re-entrainment



**FIGURE 8** | Droplets dropped on vertically placed meshes (A–C). The droplets are dispensed by a pipet with a volume of 100  $\mu\text{L}$ . Comparison of wetted meshes after fog harvesting experiments (D–F). Sequential videos of droplet motions (A–C) and water collection processes in atmospheric fog harvesting are included in **Supplementary Materials**.

occurs when the drag force is higher than the adhesion force. The analytical study gave the critical droplet radius ( $r_c$ ) for the re-entrainment [12]. If the droplet radius is higher than  $r_c$ , the droplet re-entrainment occurs. The  $r_c$  was expressed in Equation (5):

$$r_c \cong \frac{4\pi \gamma_{LV} \sin^2 \theta (1 + \cos \theta_{rec})}{\rho_{air} v_0^2 C_D (\theta - \sin \theta \cos \theta)} \quad (5)$$

The  $r_c$  depends on the contact angle and decreases with the increase of the contact angle. Therefore, the possibility of re-entrainment increased for higher contact angles under various droplet size distributions. Therefore, it appears that the reverse performance of the #20 and #40 SHBMs is caused by re-entrainment. The superhydrophilic modification induced the reduction of re-entrainment, and fully wetted water reduced the pinning force. In addition, clogged water in SHPM attracted more droplets and grew faster. These changes resulted in the improvement of fog harvesting with superhydrophilic modifications.

## Performance in Industrial Fog Harvesting

In atmospheric fog harvesting, a mesh screen is commonly installed along the direction of gravity, perpendicular to the direction of fog-laden flows, for effective draining. As with the atmospheric fog harvesting, some of the deposited droplets are re-entrained to the fog-laden flows. In addition to the re-entrainment, a part of deposited droplets may be lost when droplets detach from wires and return back to the towers by gravity, as shown in **Figure 2C**. In industrial fog harvesting with simulated cooling towers, the fog-laden flows rise, and the

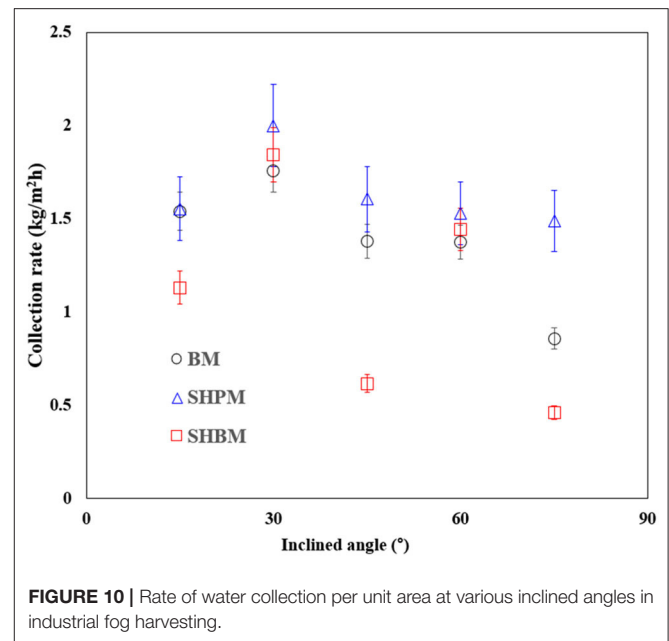
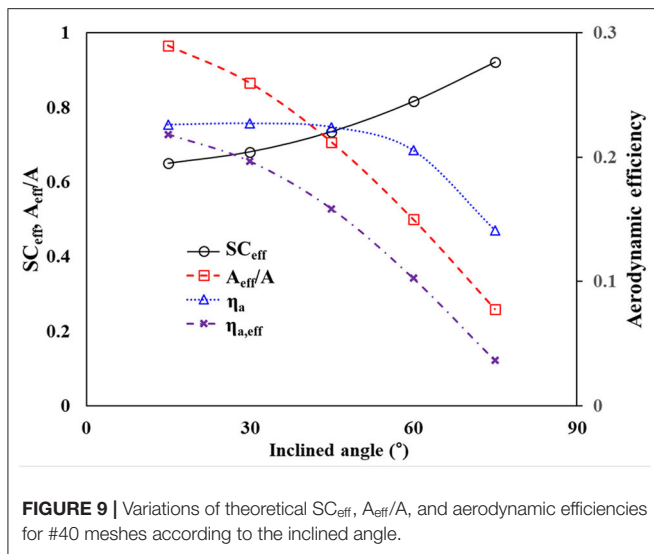
droplets that return to the towers by gravity are considered losses. In addition, the water reservoir can only be installed around the tower. Therefore, considering the drainage, it is difficult to set meshes normal to the flow direction with a flat mesh screen, and hence, the mesh screen must be tilted. In this inclined mesh, the SC can be expressed by the effective SC ( $SC_{eff}$ ), and Equation (2) is modified as shown by Ghosh et al. [2].

$$SC_{eff} = 2 \frac{\left[1 - \left(1 / \left(2D_{eff}^*\right)\right)\right]}{D_{eff}^*}, \quad (6)$$

$$\eta_a = \frac{SC_{eff}}{1 + \sqrt{\frac{C_0 \cos \theta}{C_D}}}, \quad (7)$$

where  $D_{eff}^*$  is the effective spacing ratio denoted by  $(R + D_{eff})/R$ . The effective opening  $D_{eff}$  is expressed by  $D \cos \theta$  in the spatial distance of  $2D$ . The theoretical changes in  $SC_{eff}$  and  $\eta_a$  are presented in **Figure 8**. As  $\theta$  increases,  $SC_{eff}$  increases monotonically. The corresponding  $\eta_a$  initially increases slightly and then decreases drastically.

With the assumption that uniform fog-laden flows increase directly, the effective area ( $A_{eff}$ ) of a flat mesh screen, where interactions occur between the mesh and droplets, reduces as the mesh is tilted.  $A_{eff}$  is expressed by  $A \cos \theta$ , where  $A$  is the original interactive area. This reduction must also be considered because  $\eta_a$  represents the fraction of droplets in  $A_{eff}$  only. The effective aerodynamic efficiency ( $\eta_{a,eff}$ ) can be calculated by multiplying  $A_{eff}$  and  $\eta_a$ . According to the inclined angle, the reduction of  $A_{eff}$  and the corresponding  $\eta_{a,eff}$  are represented in **Figure 9**. The #40 meshes were used in industrial fog harvesting measurements



because the #20 and #40 meshes produced similar results. Both  $A_{eff}$  and the corresponding  $\eta_{a,eff}$  decreased monotonically with increasing  $\theta$ . In practical applications, the applicable size of the mesh screens is limited. Therefore, it is more appropriate to evaluate the water harvesting performance with  $\eta_{a,eff}$ .

**Figure 10** shows the rate of water collection per unit area ( $W''_{col}$ ) in simulated industrial fog harvesting, for various  $\theta$  values. It was difficult to calculate the collection efficiency using Equation (4) because only some part of the tower exit was used, as shown in **Figure 2**, which creates ambiguity in the amount of water generated. Therefore,  $W''_{col}$  was used instead of the collection efficiency. As  $\theta$  increased,  $W''_{col}$  initially increased, had a peak value at  $30^\circ$ , and then decreased. This tendency is similar to that described in the previous study, although the optimal inclination angle is different due to the differences in SC, wire size, and generated droplet size [34]. A deposited droplet on a mesh initially grows until it has enough force to overcome the pinning force. In contrast to atmospheric water harvesting, the captured droplets had to slide along meshes to reach a reservoir. When the droplet size becomes bigger, it moves along the inclined mesh or returns to the tower by gravity, as shown in **Figure 2C**. During the sliding process, large droplets detached due to gravity and falling caused the draining loss. Regardless of the surface wettability, the best performance occurred at a  $\theta$  of  $30^\circ$ , where the theoretical  $\eta_a$  was the maximum. At low- and high- $\theta$ , the water collection performance mainly depended on the returning-back loss, because of the longer sliding length and reduction of effective area, respectively. The optimal  $\theta$  was determined as a tradeoff between these two factors. The sliding and returning are related to the adhesion force, and the force is related to the wettability. SHBM provides a smaller adhesion force compared to BM. This caused lower performance in SHBM. Compared to BM and SHBM, SHPM had a higher collecting performance at all angles of  $\theta$ . Hydrophilic wettability reduced the returning-back loss, and SHPM was more effective than other meshes.

## CONCLUSION

In this study, the effects of mesh wettability modifications on atmospheric and industrial fog harvesting were investigated experimentally. The mesh wettability was modified successfully through robust and simple methods, which were the formation of hierarchical micro/nanostructures and HDFs SAM coating. In atmospheric fog harvesting, both SHPMs and SHBMs showed higher collection efficiencies than the original mesh. The superhydrophobic treatment was the most effective because it maintained the aerodynamic characteristics of the meshes, owing to the clogging protection. In contrast, in industrial fog harvesting in simulating cooling towers, superhydrophilicity was more effective because the hydrophilic characteristic caused lower gravity-induced draining loss. In addition, when a flat mesh screen was employed in industrial fog harvesting, the optimal tilting angle was determined through a compromise between the gravity-induced draining loss and reduction of the effective area. This study will help design fog harvesting mesh screens by understanding the influence of mesh wettability modifications on the water collection performance in both atmospheric and industrial fog harvesting applications.

## DATA AVAILABILITY STATEMENT

The raw data supporting the conclusions of this article will be made available by the authors, without undue reservation.

## AUTHOR CONTRIBUTIONS

JKa, J-WL, and SJ contributed to conception and design of the study. JKa, JM, and HJ organized the database. SJ performed the statistical analysis. JKa and SJ wrote the first draft of the manuscript and wrote sections of the manuscript. All authors

contributed to manuscript revision, read, and approved the submitted version.

## FUNDING

This work was supported by a National Research Foundation (NRF) of Korea, a grant funded by the Korean government (grant number NRF-2020R1C1C1004344), and the Human Resources Program in Energy Technology of the Korea Institute of Energy Technology Evaluation and Planning (KETEP), which was granted financial resources from the Ministry of Trade, Industry & Energy, Republic of Korea (grant number 20194030202410).

## REFERENCES

- Rosegrant MW, Cai X, Cline SA. *Global water outlook to 2025*. Food policy reports 14. International Food Policy Research Institute (IFPRI) (2002).
- Ghosh R, Ray TK, Ganguly R. Cooling tower fog harvesting in power plants—A pilot study. *Energy*. (2015) 89:1018–28. doi: 10.1016/j.energy.2015.06.050
- General Assembly. *UN documents - A/RES/58/217*. Vol. A/RES/58/217. United Nations (2003).
- United Nations Educational Scientific, Paris CO. *The United Nations World Water Development Report 4, Vol. 1. Managing Water Uncertainty and Risk*. Unesco (2012).
- Beysens D, Milimouk I. The case for alternative fresh water sources. *Pour Resour Alternat Secheresse*. (2000) 11:1–16.
- Yu TS, Park J, Lim H, Breuer KS. Fog deposition and accumulation on smooth and textured hydrophobic surfaces. *Langmuir*. (2012) 28:12771–8. doi: 10.1021/la301901m
- White B, Sarkar A, Kietzig AM. Fog-harvesting inspired by the *Stenocara* beetle—An analysis of drop collection and removal from biomimetic samples with wetting contrast. *Appl Surf Sci*. (2013) 284:826–36. doi: 10.1016/j.apsusc.2013.08.017
- Yao Y, Aizenberg J, Park KC. Dropwise condensation on hydrophobic bumps and dimples. *Appl Phys Lett*. (2018) 112:151605. doi: 10.1063/1.5021343
- Al-Khayat O, Hong JK, Beck DM, Minett AL, Neto C. Patterned polymer coatings increase the efficiency of dew harvesting. *ACS Appl Mater Interf*. (2017) 9:13676–84. doi: 10.1021/acsami.6b16248
- Schemenauer RS, Joe PI. The collection efficiency of a massive fog collector. *Atmos Res*. (1989) 24:53–69. doi: 10.1016/0169-8095(89)90036-7
- Gleick PH. Water use. *Annu Rev Environ Resour*. (2003) 28:275–314. doi: 10.1146/annurev.energy.28.040202.122849
- Park KC, Chhatre SS, Srinivasan S, Cohen RE, Mckinley GH. Optimal design of permeable fiber network structures for fog harvesting. *Langmuir*. (2013) 29:13269–77. doi: 10.1021/la402409f
- Shi W, Anderson MJ, Tulkoff JB, Kennedy BS, Boreyko JB. Fog harvesting with harps. *ACS Appl Mater Interf*. (2018) 10:11979–86. doi: 10.1021/acsami.7b17488
- Jiang Y, Savarirayan S, Yao Y, Park KC. Fog collection on a superhydrophilic wire. *Appl Phys Lett*. (2019) 114:083701. doi: 10.1063/1.5087144
- Schemenauer RS, Cereceda P. A proposed standard fog collector for use in high-elevation regions. *J Appl Meteorol*. (1994) 33:1313–22. doi: 10.1175/1520-0450(1994)033<1313:APSCFC>2.0.CO;2
- Cereceda P, Larrain H, Osses P, Farias M, Egaña I. The spatial and temporal variability of fog and its relation to fog oases in the Atacama Desert, Chile. *Atmos Res*. (2008) 87:312–23. doi: 10.1016/j.atmosres.2007.11.012
- Klemm O, Schemenauer RS, Lummerich A, Cereceda P, Marzol V, Corell D, et al. Fog as a fresh-water resource: overview and perspectives. *Ambio*. (2012) 41:221–34. doi: 10.1007/s13280-012-0247-8

## SUPPLEMENTARY MATERIAL

The Supplementary Material for this article can be found online at: <https://www.frontiersin.org/articles/10.3389/fphy.2021.680641/full#supplementary-material>

**Supplementary Video 1** | Droplet on BM.

**Supplementary Video 2** | Droplet on SHPM.

**Supplementary Video 3** | Droplet on SHBM.

**Supplementary Video 4** | Atmospheric water harvesting video with BM.

**Supplementary Video 5** | Atmospheric water harvesting video with SHPM.

**Supplementary Video 6** | Atmospheric water harvesting video with SHBM.

- Rajaram M, Heng X, Oza M, Luo C. Enhancement of fog-collection efficiency of a Raschel mesh using surface coatings and local geometric changes. *Colloids Surf A Physicochem Eng Aspects*. (2016) 508:218–29. doi: 10.1016/j.colsurfa.2016.08.034
- Seo D, Lee J, Lee C, Nam Y. The effects of surface wettability on the fog and dew moisture harvesting performance on tubular surfaces. *Sci Rep*. (2016) 6:24276. doi: 10.1038/srep24276
- Andrews HG, Eccles EA, Schofield WCE, Badyal JPS. Three-Dimensional hierarchical structures for fog harvesting. *Langmuir*. (2011) 27:3798–802. doi: 10.1021/la2000014
- Bai H, Zhang C, Long Z, Geng H, Ba T, Fan Y, et al. A hierarchical hydrophilic/hydrophobic cooperative fog collector possessing self-pumped droplet delivering ability. *J Mater Chem A*. (2018) 6:20966–72. doi: 10.1039/C8TA08267G
- Chen D, Li J, Zhao J, Guo J, Zhang S, Sherazi TA, et al. Bioinspired superhydrophilic-hydrophobic integrated surface with conical pattern-shape for self-driven fog collection. *J Colloid Interf Sci*. (2018) 530:274–81. doi: 10.1016/j.jcis.2018.06.081
- Dai X, Sun N, Nielsen SO, Stogin BB, Wang J, Yang S, et al. Hydrophilic directional slippery rough surfaces for water harvesting. *Sci Adv*. (2018) 4:eaaq0919. doi: 10.1126/sciadv.aaq0919
- Gürsoy M. All-dry patterning method to fabricate hydrophilic/hydrophobic surface for fog harvesting. *Colloid Polym Sci*. (2020) 298:969–76. doi: 10.1007/s00396-020-04656-x
- Zhou H, Jing X, Guo Z. Excellent fog droplets collector via an extremely stable hybrid hydrophobic-hydrophilic surface and Janus copper foam integrative system with hierarchical micro/nanostructures. *J Colloid Interf Sci*. (2020) 561:730–40. doi: 10.1016/j.jcis.2019.11.048
- Veldhuizen H, Ledbetter J. Cooling tower fog: control and abatement. *J Air Pollut Cont Assoc*. (1971) 21:21–4. doi: 10.1080/00022470.1971.10469490
- Ghosh R, Patra C, Singh P, Ganguly R, Sahu RP, Zhitomirsky I, et al. Influence of metal mesh wettability on fog harvesting in industrial cooling towers. *Appl Therm Eng*. (2020) 181:115963. doi: 10.1016/j.applthermaleng.2020.115963
- Lee JW, Hwang W. Fabrication of a superhydrophobic surface with fungus-cleaning properties on brazed aluminum for industrial application in heat exchangers. *Appl Surf Sci*. (2018) 442:461–6. doi: 10.1016/j.apsusc.2018.02.170
- Rothman T, Ledbetter JO. Droplet size of cooling tower fog. *Environ Lett*. (1975) 10:191–203. doi: 10.1080/00139307509435821
- Seo YI, Lee YJ, Kim DG, Lee KH, Do Kim. Y. Mechanism of aluminum hydroxide layer formation by surface modification of aluminum. *Appl Surf Sci*. (2010) 256:4434–7. doi: 10.1016/j.apsusc.2010.01.011
- Cho H, Kim D, Lee C, Hwang W. A simple fabrication method for mechanically robust superhydrophobic surface by hierarchical aluminum hydroxide structures. *Curr Appl Phys*. (2013) 13:762–7. doi: 10.1016/j.cap.2012.11.021
- Rivera JDD. Aerodynamic collection efficiency of fog water collectors. *Atmos Res*. (2011) 102:335–42. doi: 10.1016/j.atmosres.2011.08.005
- Munson BR, Young DF, Okiishi TH, Huebsch WW. *Fundamentals of Fluid Mechanics*. John Wiley & Sons. Inc. (2006).

34. Ghosh R, Ganguly R. Fog harvesting from cooling towers using metal mesh: Effects of aerodynamic, deposition, drainage efficiencies. *Proc Inst Mech Eng A J Power Energy*. (2020) 234:994–1014. doi: 10.1177/0957650919890711

**Conflict of Interest:** The authors declare that the research was conducted in the absence of any commercial or financial relationships that could be construed as a potential conflict of interest.

*Copyright © 2021 Kang, Lee, Kim, Moon, Jang and Jung. This is an open-access article distributed under the terms of the Creative Commons Attribution License (CC BY). The use, distribution or reproduction in other forums is permitted, provided the original author(s) and the copyright owner(s) are credited and that the original publication in this journal is cited, in accordance with accepted academic practice. No use, distribution or reproduction is permitted which does not comply with these terms.*